



Measurements of the branching fractions and CP asymmetries of $B^\pm \rightarrow J/\psi \pi^\pm$ and $B^\pm \rightarrow \psi(2S)\pi^\pm$ decays

The LHCb collaboration ¹

Abstract

A study of $B^\pm \rightarrow J/\psi \pi^\pm$ and $B^\pm \rightarrow \psi(2S)\pi^\pm$ decays is performed with data corresponding to 0.37 fb^{-1} of proton-proton collisions at $\sqrt{s} = 7 \text{ TeV}$. Their branching fractions are found to be

$$\begin{aligned} \mathcal{B}(B^\pm \rightarrow J/\psi \pi^\pm) &= (3.88 \pm 0.11 \pm 0.15) \times 10^{-5} \text{ and} \\ \mathcal{B}(B^\pm \rightarrow \psi(2S)\pi^\pm) &= (2.52 \pm 0.26 \pm 0.15) \times 10^{-5}, \end{aligned}$$

where the first uncertainty is related to the statistical size of the sample and the second quantifies systematic effects. The measured CP asymmetries in these modes are

$$\begin{aligned} A_{CP}^{J/\psi \pi} &= 0.005 \pm 0.027 \pm 0.011 \text{ and} \\ A_{CP}^{\psi(2S)\pi} &= 0.048 \pm 0.090 \pm 0.011 \end{aligned}$$

with no evidence of direct CP violation seen.

Submitted to Phys. Rev. X

¹Authors are listed on the following pages.

LHCb collaboration

R. Aaij³⁸, C. Abellan Beteta^{33,n}, B. Adeva³⁴, M. Adinolfi⁴³, C. Adrover⁶, A. Affolder⁴⁹, Z. Ajaltouni⁵, J. Albrecht³⁵, F. Alessio³⁵, M. Alexander⁴⁸, S. Ali³⁸, G. Alkhazov²⁷, P. Alvarez Cartelle³⁴, A.A. Alves Jr²², S. Amato², Y. Amhis³⁶, J. Anderson³⁷, R.B. Appleby⁵¹, O. Aquines Gutierrez¹⁰, F. Archilli^{18,35}, A. Artamonov³², M. Artuso^{53,35}, E. Aslanides⁶, G. Auriemma^{22,m}, S. Bachmann¹¹, J.J. Back⁴⁵, V. Balagura^{28,35}, W. Baldini¹⁶, R.J. Barlow⁵¹, C. Barschel³⁵, S. Barsuk⁷, W. Barter⁴⁴, A. Bates⁴⁸, C. Bauer¹⁰, Th. Bauer³⁸, A. Bay³⁶, I. Bediaga¹, S. Belogurov²⁸, K. Belous³², I. Belyaev²⁸, E. Ben-Haim⁸, M. Benayoun⁸, G. Bencivenni¹⁸, S. Benson⁴⁷, J. Benton⁴³, R. Bernet³⁷, M.-O. Bettler¹⁷, M. van Beuzekom³⁸, A. Bien¹¹, S. Bifani¹², T. Bird⁵¹, A. Bizzeti^{17,h}, P.M. Bjørnstad⁵¹, T. Blake³⁵, F. Blanc³⁶, C. Blanks⁵⁰, J. Blouw¹¹, S. Blusk⁵³, A. Bobrov³¹, V. Bocci²², A. Bondar³¹, N. Bondar²⁷, W. Bonivento¹⁵, S. Borghi^{48,51}, A. Borgia⁵³, T.J.V. Bowcock⁴⁹, C. Bozzi¹⁶, T. Brambach⁹, J. van den Brand³⁹, J. Bressieux³⁶, D. Brett⁵¹, M. Britsch¹⁰, T. Britton⁵³, N.H. Brook⁴³, H. Brown⁴⁹, K. de Bruyn³⁸, A. Büchler-Germann³⁷, I. Burducea²⁶, A. Bursche³⁷, J. Buytaert³⁵, S. Cadeddu¹⁵, O. Callot⁷, M. Calvi^{20,j}, M. Calvo Gomez^{33,n}, A. Camboni³³, P. Campana^{18,35}, A. Carbone¹⁴, G. Carboni^{21,k}, R. Cardinale^{19,i,35}, A. Cardini¹⁵, L. Carson⁵⁰, K. Carvalho Akiba², G. Casse⁴⁹, M. Cattaneo³⁵, Ch. Cauet⁹, M. Charles⁵², Ph. Charpentier³⁵, N. Chiapolini³⁷, K. Ciba³⁵, X. Cid Vidal³⁴, G. Ciezarek⁵⁰, P.E.L. Clarke^{47,35}, M. Clemencic³⁵, H.V. Cliff⁴⁴, J. Closier³⁵, C. Coca²⁶, V. Coco³⁸, J. Cogan⁶, P. Collins³⁵, A. Comerma-Montells³³, A. Contu⁵², A. Cook⁴³, M. Coombes⁴³, G. Corti³⁵, B. Couturier³⁵, G.A. Cowan³⁶, R. Currie⁴⁷, C. D'Ambrosio³⁵, P. David⁸, P.N.Y. David³⁸, I. De Bonis⁴, S. De Capua^{21,k}, M. De Cian³⁷, J.M. De Miranda¹, L. De Paula², P. De Simone¹⁸, D. Decamp⁴, M. Deckenhoff⁹, H. Degaudenzi^{36,35}, L. Del Buono⁸, C. Deplano¹⁵, D. Derkach^{14,35}, O. Deschamps⁵, F. Detori³⁹, J. Dickens⁴⁴, H. Dijkstra³⁵, P. Diniz Batista¹, F. Domingo Bonal^{33,n}, S. Donleavy⁴⁹, F. Dordei¹¹, A. Dotti Suárez³⁴, D. Dossett⁴⁵, A. Dovbnya⁴⁰, F. Dupertuis³⁶, R. Dzhelyadin³², A. Dziurda²³, S. Easo⁴⁶, U. Egede⁵⁰, V. Egorychev²⁸, S. Eidelman³¹, D. van Eijk³⁸, F. Eisele¹¹, S. Eisenhardt⁴⁷, R. Ekelhof⁹, L. Eklund⁴⁸, Ch. Elsasser³⁷, D. Elsby⁴², D. Esperante Pereira³⁴, A. Falabella^{16,e,14}, C. Färber¹¹, G. Fardell⁴⁷, C. Farinelli³⁸, S. Farry¹², V. Fave³⁶, V. Fernandez Albor³⁴, M. Ferro-Luzzi³⁵, S. Filippov³⁰, C. Fitzpatrick⁴⁷, M. Fontana¹⁰, F. Fontanelli^{19,i}, R. Forty³⁵, O. Francisco², M. Frank³⁵, C. Frei³⁵, M. Frosini^{17,f}, S. Furcas²⁰, A. Gallas Torreira³⁴, D. Galli^{14,c}, M. Gandelman², P. Gandini⁵², Y. Gao³, J.-C. Garnier³⁵, J. Garofoli⁵³, J. Garra Tico⁴⁴, L. Garrido³³, D. Gascon³³, C. Gaspar³⁵, R. Gauld⁵², N. Gauvin³⁶, M. Gersabeck³⁵, T. Gershon^{45,35}, Ph. Ghez⁴, V. Gibson⁴⁴, V.V. Gligorov³⁵, C. Göbel⁵⁴, D. Golubkov²⁸, A. Golutvin^{50,28,35}, A. Gomes², H. Gordon⁵², M. Grabalosa Gándara³³, R. Graciani Diaz³³, L.A. Granado Cardoso³⁵, E. Graugés³³, G. Graziani¹⁷, A. Grecu²⁶, E. Greening⁵², S. Gregson⁴⁴, B. Gui⁵³, E. Gushchin³⁰, Yu. Guz³², T. Gys³⁵, C. Hadjivasiliou⁵³, G. Haefeli³⁶, C. Haen³⁵, S.C. Haines⁴⁴, T. Hampson⁴³, S. Hansmann-Menzener¹¹, R. Harji⁵⁰, N. Harnew⁵², J. Harrison⁵¹, P.F. Harrison⁴⁵, T. Hartmann⁵⁵, J. He⁷, V. Heijne³⁸, K. Hennessy⁴⁹, P. Henrard⁵, J.A. Hernando Morata³⁴, E. van Herwijnen³⁵, E. Hicks⁴⁹, K. Holubyev¹¹, P. Hopchev⁴, W. Hulsbergen³⁸, P. Hunt⁵², T. Huse⁴⁹, R.S. Huston¹², D. Hutchcroft⁴⁹, D. Hynds⁴⁸, V. Iakovenko⁴¹, P. Ilten¹², J. Imong⁴³, R. Jacobsson³⁵, A. Jaeger¹¹, M. Jahjah Hussein⁵, E. Jans³⁸, F. Jansen³⁸, P. Jaton³⁶, B. Jean-Marie⁷, F. Jing³, M. John⁵², D. Johnson⁵², C.R. Jones⁴⁴, B. Jost³⁵, M. Kaballo⁹, S. Kandybei⁴⁰, M. Karacson³⁵, T.M. Karbach⁹, J. Keaveney¹², I.R. Kenyon⁴², U. Kerzel³⁵, T. Ketel³⁹, A. Keune³⁶, B. Khanji⁶, Y.M. Kim⁴⁷, M. Knecht³⁶, R.F. Koopman³⁹, P. Koppenburg³⁸, M. Korolev²⁹, A. Kozlinskiy³⁸, L. Kravchuk³⁰, K. Kreplin¹¹, M. Krepis⁴⁵, G. Krocker¹¹, P. Krokovny¹¹, F. Kruse⁹, K. Kruzelecki³⁵, M. Kucharczyk^{20,23,35,j}, V. Kudryavtsev³¹, T. Kvaratskheliya^{28,35}, V.N. La Thi³⁶, D. Lacarrere³⁵, G. Lafferty⁵¹, A. Lai¹⁵, D. Lambert⁴⁷, R.W. Lambert³⁹, E. Lanciotti³⁵, G. Lanfranchi¹⁸, C. Langenbruch¹¹, T. Latham⁴⁵, C. Lazzeroni⁴², R. Le Gac⁶, J. van Leerdam³⁸, J.-P. Lees⁴, R. Lefèvre⁵, A. Leflat^{29,35}, J. Lefrançois⁷, O. Leroy⁶, T. Lesiak²³, L. Li³, L. Li Gioi⁵, M. Lieng⁹, M. Liles⁴⁹, R. Lindner³⁵, C. Linn¹¹, B. Liu³, G. Liu³⁵, J. von Loeben²⁰, J.H. Lopes², E. Lopez Asamar³³, N. Lopez-March³⁶, H. Lu³, J. Luisier³⁶, A. Mac Raighne⁴⁸, F. Machefert⁷, I.V. Machikhiliyan^{4,28}, F. Maciuc¹⁰, O. Maev^{27,35}, J. Magnin¹, S. Malde⁵², R.M.D. Mamunur³⁵, G. Manca^{15,d}, G. Mancinelli⁶, N. Mangiafave⁴⁴, U. Marconi¹⁴, R. Märki³⁶, J. Marks¹¹, G. Martellotti²², A. Martens⁸, L. Martin⁵², A. Martín Sánchez⁷, M. Martinelli³⁸, D. Martinez Santos³⁵, A. Massafferri¹, Z. Mathe¹², C. Matteuzzi²⁰, M. Matveev²⁷, E. Maurice⁶, B. Maynard⁵³, A. Mazurov^{16,30,35}, G. McGregor⁵¹, R. McNulty¹², M. Meissner¹¹, M. Merk³⁸, J. Merkel⁹, S. Miglioranza³⁵, D.A. Milanes¹³, M.-N. Minard⁴, J. Molina Rodriguez⁵⁴, S. Monteil⁵, D. Moran¹², P. Morawski²³, R. Mountain⁵³, I. Mous³⁸, F. Muheim⁴⁷, K. Müller³⁷, R. Muresan²⁶, B. Muryn²⁴, B. Muster³⁶, J. Mylroie-Smith⁴⁹, P. Naik⁴³, T. Nakada³⁶, R. Nandakumar⁴⁶, I. Nasteva¹, M. Needham⁴⁷, N. Neufeld³⁵, A.D. Nguyen³⁶, C. Nguyen-Mau^{36,o}, M. Nicol⁷, V. Niess⁵, N. Nikitin²⁹, A. Nomerotski^{52,35}, A. Novoselov³², A. Oblakowska-Mucha²⁴, V. Obraztsov³², S. Oggero³⁸, S. Ogilvy⁴⁸, O. Okhrimenko⁴¹, R. Oldeman^{15,d,35}, M. Orlowska²⁶, J.M. Otalora Goicochea², P. Owen⁵⁰, K. Pal⁵³, J. Palacios³⁷, A. Palano^{13,b}, M. Palutan¹⁸, J. Panman³⁵, A. Papanestis⁴⁶, M. Pappagallo⁴⁸, C. Parkes⁵¹, C.J. Parkinson⁵⁰, G. Passaleva¹⁷, G.D. Patel⁴⁹, M. Patel⁵⁰, S.K. Paterson⁵⁰, G.N. Patrick⁴⁶, C. Patrignani^{19,i}, C. Pavel-Nicorescu²⁶, A. Pazos Alvarez³⁴,

A. Pellegrino³⁸, G. Penso^{22,l}, M. Pepe Altarelli³⁵, S. Perazzini^{14,c}, D.L. Perego^{20,j}, E. Perez Trigo³⁴, A. Pérez-Calero Yzquierdo³³, P. Perret⁵, M. Perrin-Terrin⁶, G. Pessina²⁰, A. Petrolini^{19,i}, A. Phan⁵³, E. Picatoste Olloqui³³, B. Pie Valls³³, B. Pietrzyk⁴, T. Pilar⁴⁵, D. Pinci²², R. Plackett⁴⁸, S. Playfer⁴⁷, M. Plo Casasus³⁴, G. Polok²³, A. Poluektov^{45,31}, E. Polcarpo², D. Popov¹⁰, B. Popovici²⁶, C. Potterat³³, A. Powell⁵², J. Prisciandaro³⁶, V. Pugatch⁴¹, A. Puig Navarro³³, W. Qian⁵³, J.H. Rademacker⁴³, B. Rakotomiamanana³⁶, M.S. Rangel², I. Raniuk⁴⁰, G. Raven³⁹, S. Redford⁵², M.M. Reid⁴⁵, A.C. dos Reis¹, S. Ricciardi⁴⁶, A. Richards⁵⁰, K. Rinnert⁴⁹, D.A. Roa Romero⁵, P. Robbe⁷, E. Rodrigues^{48,51}, F. Rodrigues², P. Rodriguez Perez³⁴, G.J. Rogers⁴⁴, S. Roiser³⁵, V. Romanovsky³², M. Rosello^{33,n}, J. Rouvinet³⁶, T. Ruf³⁵, H. Ruiz³³, G. Sabatino^{21,k}, J.J. Saborido Silva³⁴, N. Sagidova²⁷, P. Sail⁴⁸, B. Saitta^{15,d}, C. Salzmann³⁷, M. Sannino^{19,i}, R. Santacesaria²², C. Santamarina Rios³⁴, R. Santinelli³⁵, E. Santovetti^{21,k}, M. Sapunov⁶, A. Sarti^{18,l}, C. Satriano^{22,m}, A. Satta²¹, M. Savrie^{16,e}, D. Savrina²⁸, P. Schaack⁵⁰, M. Schiller³⁹, H. Schindler³⁵, S. Schleich⁹, M. Schlupp⁹, M. Schmelling¹⁰, B. Schmidt³⁵, O. Schneider³⁶, A. Schopper³⁵, M.-H. Schune⁷, R. Schwemmer³⁵, B. Sciascia¹⁸, A. Sciubba^{18,l}, M. Seco³⁴, A. Semennikov²⁸, K. Senderowska²⁴, I. Sepp⁵⁰, N. Serra³⁷, J. Serrano⁶, P. Seyfert¹¹, M. Shapkin³², I. Shapoval^{40,35}, P. Shatalov²⁸, Y. Shcheglov²⁷, T. Shears⁴⁹, L. Shekhtman³¹, O. Shevchenko⁴⁰, V. Shevchenko²⁸, A. Shires⁵⁰, R. Silva Coutinho⁴⁵, T. Skwarnicki⁵³, N.A. Smith⁴⁹, E. Smith^{52,46}, K. Sobczak⁵, F.J.P. Soler⁴⁸, A. Solomin⁴³, F. Soomro^{18,35}, B. Souza De Paula², B. Spaan⁹, A. Sparkes⁴⁷, P. Spradlin⁴⁸, F. Stagni³⁵, S. Stahl¹¹, O. Steinkamp³⁷, S. Stoica²⁶, S. Stone^{53,35}, B. Storaci³⁸, M. Straticiu²⁶, U. Straumann³⁷, V.K. Subbiah³⁵, S. Swientek⁹, M. Szczekowski²⁵, P. Szczypka³⁶, T. Szumlak²⁴, S. T'Jampens⁴, E. Teodorescu²⁶, F. Teubert³⁵, C. Thomas⁵², E. Thomas³⁵, J. van Tilburg¹¹, V. Tisserand⁴, M. Tobin³⁷, S. Topp-Joergensen⁵², N. Torr⁵², E. Tournefier^{4,50}, S. Tourneur³⁶, M.T. Tran³⁶, A. Tsaregorodtsev⁶, N. Tuning³⁸, M. Ubeda Garcia³⁵, A. Ukleja²⁵, U. Uwer¹¹, V. Vagnoni¹⁴, G. Valenti¹⁴, R. Vazquez Gomez³³, P. Vazquez Regueiro³⁴, S. Vecchi¹⁶, J.J. Velthuis⁴³, M. Veltri^{17,9}, B. Viaud⁷, I. Videau⁷, D. Vieira², X. Vilasis-Cardona^{33,n}, J. Visniakov³⁴, A. Vollhardt³⁷, D. Volyanskyy¹⁰, D. Voong⁴³, A. Vorobyev²⁷, H. Voss¹⁰, R. Waldi⁵⁵, S. Wandernoth¹¹, J. Wang⁵³, D.R. Ward⁴⁴, N.K. Watson⁴², A.D. Webber⁵¹, D. Websdale⁵⁰, M. Whitehead⁴⁵, D. Wiedner¹¹, L. Wiggers³⁸, G. Wilkinson⁵², M.P. Williams^{45,46}, M. Williams⁵⁰, F.F. Wilson⁴⁶, J. Wishahi⁹, M. Witek²³, W. Witzeling³⁵, S.A. Wotton⁴⁴, K. Wyllie³⁵, Y. Xie⁴⁷, F. Xing⁵², Z. Xing⁵³, Z. Yang³, R. Young⁴⁷, O. Yushchenko³², M. Zangoli¹⁴, M. Zavertyaev^{10,a}, F. Zhang³, L. Zhang⁵³, W.C. Zhang¹², Y. Zhang³, A. Zhelezov¹¹, L. Zhong³, A. Zvyagin³⁵.

¹ Centro Brasileiro de Pesquisas Físicas (CBPF), Rio de Janeiro, Brazil

² Universidade Federal do Rio de Janeiro (UFRJ), Rio de Janeiro, Brazil

³ Center for High Energy Physics, Tsinghua University, Beijing, China

⁴ LAPP, Université de Savoie, CNRS/IN2P3, Annecy-Le-Vieux, France

⁵ Clermont Université, Université Blaise Pascal, CNRS/IN2P3, LPC, Clermont-Ferrand, France

⁶ CPPM, Aix-Marseille Université, CNRS/IN2P3, Marseille, France

⁷ LAL, Université Paris-Sud, CNRS/IN2P3, Orsay, France

⁸ LPNHE, Université Pierre et Marie Curie, Université Paris Diderot, CNRS/IN2P3, Paris, France

⁹ Fakultät Physik, Technische Universität Dortmund, Dortmund, Germany

¹⁰ Max-Planck-Institut für Kernphysik (MPIK), Heidelberg, Germany

¹¹ Physikalisches Institut, Ruprecht-Karls-Universität Heidelberg, Heidelberg, Germany

¹² School of Physics, University College Dublin, Dublin, Ireland

¹³ Sezione INFN di Bari, Bari, Italy

¹⁴ Sezione INFN di Bologna, Bologna, Italy

¹⁵ Sezione INFN di Cagliari, Cagliari, Italy

¹⁶ Sezione INFN di Ferrara, Ferrara, Italy

¹⁷ Sezione INFN di Firenze, Firenze, Italy

¹⁸ Laboratori Nazionali dell'INFN di Frascati, Frascati, Italy

¹⁹ Sezione INFN di Genova, Genova, Italy

²⁰ Sezione INFN di Milano Bicocca, Milano, Italy

²¹ Sezione INFN di Roma Tor Vergata, Roma, Italy

²² Sezione INFN di Roma La Sapienza, Roma, Italy

²³ Henryk Niewodniczanski Institute of Nuclear Physics Polish Academy of Sciences, Kraków, Poland

²⁴ AGH University of Science and Technology, Kraków, Poland

²⁵ Soltan Institute for Nuclear Studies, Warsaw, Poland

²⁶ Horia Hulubei National Institute of Physics and Nuclear Engineering, Bucharest-Magurele, Romania

²⁷ Petersburg Nuclear Physics Institute (PNPI), Gatchina, Russia

²⁸ Institute of Theoretical and Experimental Physics (ITEP), Moscow, Russia

²⁹ Institute of Nuclear Physics, Moscow State University (SINP MSU), Moscow, Russia

³⁰ Institute for Nuclear Research of the Russian Academy of Sciences (INR RAN), Moscow, Russia

³¹ Budker Institute of Nuclear Physics (SB RAS) and Novosibirsk State University, Novosibirsk, Russia

³² Institute for High Energy Physics (IHEP), Protvino, Russia

³³ Universitat de Barcelona, Barcelona, Spain

³⁴ Universidad de Santiago de Compostela, Santiago de Compostela, Spain

- ³⁵European Organization for Nuclear Research (CERN), Geneva, Switzerland
³⁶Ecole Polytechnique Fédérale de Lausanne (EPFL), Lausanne, Switzerland
³⁷Physik-Institut, Universität Zürich, Zürich, Switzerland
³⁸Nikhef National Institute for Subatomic Physics, Amsterdam, The Netherlands
³⁹Nikhef National Institute for Subatomic Physics and Vrije Universiteit, Amsterdam, The Netherlands
⁴⁰NSC Kharkiv Institute of Physics and Technology (NSC KIPT), Kharkiv, Ukraine
⁴¹Institute for Nuclear Research of the National Academy of Sciences (KINR), Kyiv, Ukraine
⁴²University of Birmingham, Birmingham, United Kingdom
⁴³H.H. Wills Physics Laboratory, University of Bristol, Bristol, United Kingdom
⁴⁴Cavendish Laboratory, University of Cambridge, Cambridge, United Kingdom
⁴⁵Department of Physics, University of Warwick, Coventry, United Kingdom
⁴⁶STFC Rutherford Appleton Laboratory, Didcot, United Kingdom
⁴⁷School of Physics and Astronomy, University of Edinburgh, Edinburgh, United Kingdom
⁴⁸School of Physics and Astronomy, University of Glasgow, Glasgow, United Kingdom
⁴⁹Oliver Lodge Laboratory, University of Liverpool, Liverpool, United Kingdom
⁵⁰Imperial College London, London, United Kingdom
⁵¹School of Physics and Astronomy, University of Manchester, Manchester, United Kingdom
⁵²Department of Physics, University of Oxford, Oxford, United Kingdom
⁵³Syracuse University, Syracuse, NY, United States
⁵⁴Pontifícia Universidade Católica do Rio de Janeiro (PUC-Rio), Rio de Janeiro, Brazil, associated to ²
⁵⁵Physikalisches Institut, Universität Rostock, Rostock, Germany, associated to ¹¹

^aP.N. Lebedev Physical Institute, Russian Academy of Science (LPI RAS), Moscow, Russia

^bUniversità di Bari, Bari, Italy

^cUniversità di Bologna, Bologna, Italy

^dUniversità di Cagliari, Cagliari, Italy

^eUniversità di Ferrara, Ferrara, Italy

^fUniversità di Firenze, Firenze, Italy

^gUniversità di Urbino, Urbino, Italy

^hUniversità di Modena e Reggio Emilia, Modena, Italy

ⁱUniversità di Genova, Genova, Italy

^jUniversità di Milano Bicocca, Milano, Italy

^kUniversità di Roma Tor Vergata, Roma, Italy

^lUniversità di Roma La Sapienza, Roma, Italy

^mUniversità della Basilicata, Potenza, Italy

ⁿLIFAELS, La Salle, Universitat Ramon Llull, Barcelona, Spain

^oHanoi University of Science, Hanoi, Viet Nam

The Cabibbo-suppressed decay $B^+ \rightarrow \psi\pi^+$, where ψ represents either a J/ψ or $\psi(2S)$, proceeds via a $b \rightarrow c\bar{c}d$ quark transition. Its branching fraction is expected to be about 5% of the favoured $b \rightarrow c\bar{c}s$ mode, $B^+ \rightarrow \psi K^+$ (charge conjugation is implied unless otherwise stated). The Standard Model predicts that for $b \rightarrow c\bar{c}s$ decays the tree and penguin contributions have the same weak phase and thus no direct CP violation is expected in $B^+ \rightarrow \psi K^+$. For $B^+ \rightarrow \psi\pi^+$, the tree and penguin contributions have different phases and CP asymmetries at the per mille level may occur [1]. An additional asymmetry may be generated, at the percent level, from long-distance rescattering, particularly from decays that have the same quark content ($D^0 D^-$, $D^{*-} D^0$, ...) [2]. Any asymmetry larger than this would be of significant interest.

In this paper, the CP asymmetries

$$A^{\psi\pi} = \frac{\mathcal{B}(B^- \rightarrow \psi\pi^-) - \mathcal{B}(B^+ \rightarrow \psi\pi^+)}{\mathcal{B}(B^- \rightarrow \psi\pi^-) + \mathcal{B}(B^+ \rightarrow \psi\pi^+)} \quad (1)$$

and charge-averaged ratios of branching fractions

$$R^\psi = \frac{\mathcal{B}(B^\pm \rightarrow \psi\pi^\pm)}{\mathcal{B}(B^\pm \rightarrow \psi K^\pm)} \quad (2)$$

are measured with the ψ reconstructed in the $\mu^+\mu^-$ final state. From the latter, $\mathcal{B}(B^\pm \rightarrow \psi\pi^\pm)$ may be deduced using the established $B^\pm \rightarrow \psi K^\pm$ branching fractions [3]. The CP asymmetry for $B^+ \rightarrow \psi(2S)K^+$ is also reported. $B^+ \rightarrow J/\psi K^+$ acts as a control mode in the asymmetry analysis because it is well measured and no CP violation is observed [3]. Previous measurements of the $B^+ \rightarrow J/\psi\pi^+$ branching fractions and CP asymmetries [4, 5] have an accuracy of about 10%. The $B^+ \rightarrow \psi(2S)h^+$ ($h = K, \pi$) system is less precisely known due to a factor ten lower branching fraction to the $h\mu\mu$ final state. The world average for $A^{\psi(2S)K}$ is -0.025 ± 0.024 [3] and there has been one measurement of $A^{\psi(2S)\pi} = 0.022 \pm 0.086$ [6].

The LHCb experiment [7] takes advantage of the high $b\bar{b}$ and $c\bar{c}$ cross sections at the Large Hadron Collider to record unprecedented samples of heavy hadron decays. It instruments the pseudorapidity range $2 < \eta < 5$ of the proton-proton (pp) collisions with a dipole magnet and a tracking system which achieves a momentum resolution of 0.4–0.6% in the range 5–100 GeV/ c . The dipole magnet can be operated in either polarity and this feature is used to reduce systematic effects due to detector asymmetries. In the sample analysed

here, 55% of data was taken with one polarity, 45% with the other.

The pp collisions take place inside a silicon-strip vertex detector which has active material 8 mm from the beam line. It provides measurements of track impact parameters (IP) with respect to primary collision vertices (PV) and precise reconstruction of secondary B^+ vertices. Downstream muon stations identify muons by their penetration through layers of iron shielding. Charged particle identification (PID) is realised using ring-imaging Cherenkov (RICH) detectors with three radiators: aerogel, C_4F_{10} and CF_4 . Events with a high transverse energy cluster in calorimeters or a high transverse momentum (p_T) muon activate a hardware trigger. About 1 MHz of such events are passed to a software-implemented high level trigger, which retains about 3 kHz.

The analysis is performed using 0.37 fb $^{-1}$ of data recorded by LHCb in the first half of 2011. The decay chain $B^+ \rightarrow \psi h^+$, $\psi \rightarrow \mu^+\mu^-$ is reconstructed from good quality tracks which have a track-fit χ^2 per degree of freedom < 5 . The muons are required to have momentum, $p > 3$ GeV/ c , and $p_T > 0.5$ GeV/ c . Selected hadrons have $p > 5$ GeV/ c and $p_T > 1$ GeV/ c . The two muon candidates are used to form a ψ resonance with vertex-fit $\chi^2 < 10$. The dimuon invariant mass is required to be within $^{+30}_{-40}$ MeV/ c^2 of the nominal ψ mass [3]; the asymmetric limits allow for a radiative tail.

The reconstructed B^+ candidate vertex is required to be of good quality with a vertex-fit $\chi^2 < 10$. It is ensured to originate from a PV by requiring $\chi_{IP}^2 < 25$ where the χ^2 considers the uncertainty on track IP and the PV position. In addition, the angle between the B^+ momentum vector and its direction of flight from the PV must be < 32 (10) mrad for $\psi(2S)h^+$ ($J/\psi h^+$). Furthermore, neither the muons nor the hadron track may point back to any primary vertex with $\chi_{IP}^2 < 4$. It is required that the hardware trigger accepted a muon from the B^+ candidate or by activity in the rest of the event. Hardware-trigger decisions based on the hadron are neglected to remove dependence on the correct emulation of the calorimeter's response to pions and kaons.

The B^+ candidates are refitted [8] requiring all three tracks to originate from the same point in

space and the ψ candidates to have their nominal mass [3]. Candidates for which one muon gives rise to two tracks in the reconstruction, one of which is then assumed to be the hadron, form an artificial peaking background in the $\psi(2S)h^+$ analysis. These candidates peak in the invariant mass distribution of the same-sign muon-pion combination at $m_{\mu\pi} \sim 245 \text{ MeV}/c^2$, i.e. the sum of the muon and pion rest masses. Requiring $m_{\mu\pi} > 300 \text{ MeV}/c^2$ removes this background. In 2% of events two B^+ candidates are found. If they decay within 2 mm of each other the candidate with the poorest quality vertex is removed; otherwise both are kept.

When selecting $J/\psi h^+$ candidates, a requirement is made on the decay angle of the charged hadron as measured in the rest frame of the B^+ with respect to the B^+ trajectory in the laboratory frame, $\cos(\theta_h^*) < 0$. This requires the hadron to have flown counter to the trajectory of the B^+ candidate, hence lowering its average momentum in the laboratory frame. At lower momentum, the pion-kaon mass difference provides sufficient separation in the B^+ invariant mass distribution, as shown in Fig. 1. In the $B^+ \rightarrow \psi(2S)h^+$ analysis, the average momentum of the hadrons is lower, so such a cut is unnecessary to separate the two modes.

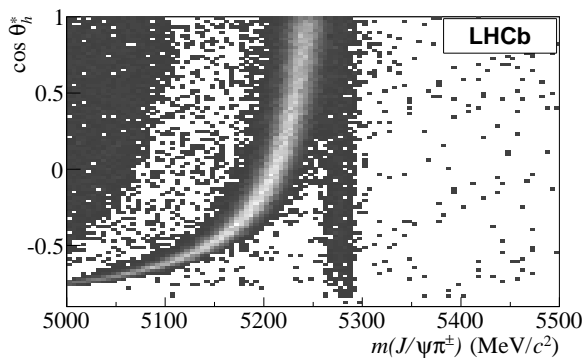


Figure 1: Distribution of $\cos(\theta_h^*)$ versus the invariant mass of $B^+ \rightarrow J/\psi \pi^+$ candidates. The curved structure contains misidentified $B^+ \rightarrow J/\psi K^+$ decays which separate from the $B^+ \rightarrow J/\psi \pi^+$ vertical band for $\cos(\theta_h^*) < 0$. The partially reconstructed background, $B \rightarrow J/\psi K \pi$ enters top left.

Particle identification information is quantified as differences between the logarithm of likelihoods, $\ln \mathcal{L}_h$, under five mass hypotheses, $h \in \{\pi, K, p, e, \mu\}$. Separation of $\psi\pi^+$ candi-

dates from ψK^+ is ensured by requiring that the hadron track satisfies $\ln \mathcal{L}_K - \ln \mathcal{L}_\pi = \text{DLL}_{K\pi} < 6$. This value is chosen to ensure that most ($\sim 95\%$) $B^+ \rightarrow \psi\pi^+$ decays are reconstructed as such. These events form the “pion-like” sample, as opposed to the kaon-like events satisfying $\text{DLL}_{K\pi} > 6$ that are reconstructed under the ψK^+ hypothesis.

The selected data are partitioned by magnet polarity, charge and $\text{DLL}_{K\pi}$ of the hadron track. By keeping the two magnet polarity samples separate, residual detection asymmetries between the left and right sides of the detector can be evaluated and hence factor out. Event yields are extracted by performing an unbinned, maximum-likelihood fit simultaneously to the eight distributions of B invariant mass in the range $5000 < m_B < 5780 \text{ MeV}/c^2$ [9]. Figure 2 shows this fit to the data for $B^+ \rightarrow J/\psi h^+$, summed over magnet polarity. The $B^+ \rightarrow \psi(2S)h^+$ data is shown in Fig. 3.

The probability density function (PDF) used to describe these distributions has several components. The correctly reconstructed, $B^+ \rightarrow \psi h^+$ events are modelled by the function,

$$f(x) \propto \exp\left(\frac{-(x - \mu)^2}{2\sigma^2 + (x - \mu)^2 \alpha_{L,R}}\right) \quad (3)$$

which describes an asymmetric peak of mean μ and width σ , and where $\alpha_L(x < \mu)$ and $\alpha_R(x > \mu)$ parameterise the tails. The mean is required to be the same for ψK^+ and $\psi\pi^+$ though it can vary across the four charge \times polarity subsamples to account for different misalignment effects. Table 1 shows the fitted values of the common tail parameters and the widths of the $B^+ \rightarrow \psi h^+$ peaks averaged over the subsamples.

Table 1: Signal shape parameters from the $B^\pm \rightarrow \psi h^\pm$ fits.

		J/ψ	$\psi(2S)$
$\sigma_{\psi K}$	(MeV/c^2)	7.84 ± 0.04	6.02 ± 0.08
$\sigma_{\psi\pi}$	(MeV/c^2)	8.58 ± 0.27	6.12 ± 0.75
α_L		0.12 ± 0.03	0.14 ± 0.01
α_R		0.10 ± 0.03	0.13 ± 0.01

The misidentified ψK^+ events form a displaced peaking structure to the left of the $\psi\pi^+$ signal and tapers to lower mass. This is modelled by a Crystal Ball function [10] which is found to be a suitable effective PDF. Its yield is added to that

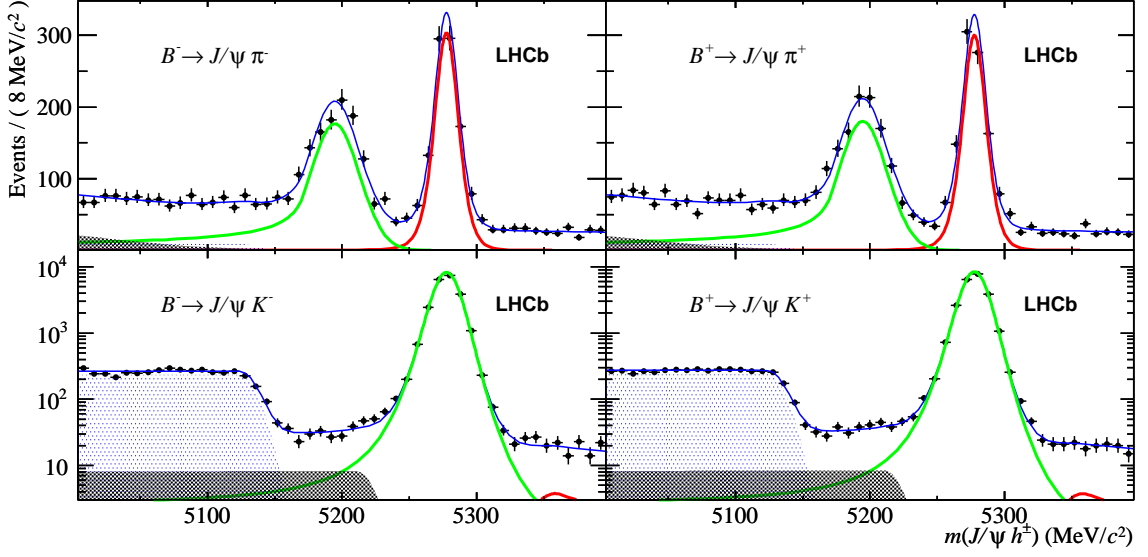


Figure 2: Distributions of $B^\pm \rightarrow J/\psi h^\pm$ invariant mass, overlain by the total fitted PDF (thin line). Pion-like events, with $DLL_{K\pi} < 6$ are reconstructed as $J/\psi \pi^\pm$ and enter in the top plots. All other events are reconstructed as $J/\psi K^\pm$ and are shown in the bottom plots on a logarithmic scale. B^- decays are shown on the left, B^+ on the right. The dark [red] curve shows the $B^\pm \rightarrow J/\psi \pi^\pm$ component, the light [green] curve represents $B^\pm \rightarrow J/\psi K^\pm$. The partially reconstructed contributions are shaded. In the lower plots these are visualised with a dark (light) shade for B_s^0 (B^+ or B^0) decays. In the top plots the shaded component are contributions from $B \rightarrow J/\psi K^\pm \pi$ (dark) and $B \rightarrow J/\psi \pi^\pm \pi$ (light).

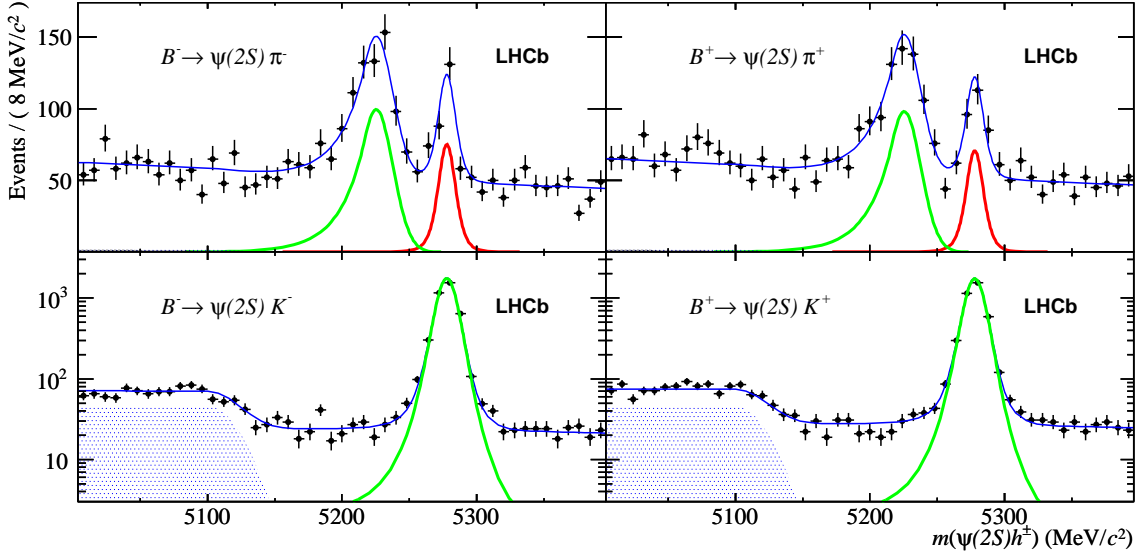


Figure 3: Distributions of $B^\pm \rightarrow \psi(2S)h^\pm$ invariant mass. See the caption of Fig. 2 for details. The partially reconstructed background in the pion-like sample is present but negligible yields are found.

of the correctly identified events to calculate the total number of ψK^+ events.

The PDF modelling the small component of $\psi\pi^+$ decays with $\text{DLL}_{K\pi} > 6$ is fixed entirely from simulation. It contributes negligibly to the total likelihood so the yield must be fixed with respect to that of correctly identified $\psi\pi^+$ events. The efficiency of the PID cut is estimated using samples of pions and kaons from $D^0 \rightarrow K^+\pi^-$ decays which are selected with high purity without using PID information. These calibration events are reweighted in bins of momentum to match the momentum distribution of the large $J/\psi K^+$ and $\psi(2S)K^+$ samples. By this technique, the following efficiencies are deduced for $\text{DLL}_{K\pi} < 6$: $\epsilon_{J/\psi\pi} = (95.8 \pm 1.0)\%$; $\epsilon_{\psi(2S)\pi} = (96.6 \pm 1.0)\%$. The errors, estimated from simulation, account for imperfections in the reweighting and the difference of the signal K^+ and π^+ momenta.

Partially reconstructed decays populate the region below the B^+ mass. $B^{+0} \rightarrow \psi K^+\pi$ decays, where the pion is missed, are modelled in the kaon-like sample by a flat PDF with a Gaussian edge. A small $\bar{B}_s^0 \rightarrow \psi K^+\pi^-$ component is needed to achieve a stable fit. It is modelled with the same shape as the partially reconstructed B^{+0} decays except shifted in mass by the B_s^0 - B^0 mass difference, $+87 \text{ MeV}/c^2$. In the pion-like sample, $\psi\pi^+\pi$ backgrounds are assumed to enter with the same PDF, and same proportion relative to the signal, as the $\psi K^+\pi$ background in the kaon-like sample. A component of misidentified $B^{+0} \rightarrow J/\psi K^+\pi$ is also included with a fixed shape estimated from the data. Lastly, a linear polynomial with a negative gradient is used to approximate the combinatorial background. The slope of this component of the pion-like and kaon-like backgrounds can differ.

The stability of the fit is tested with a large sample of pseudo-experiments. Pull distributions from these tests are consistent with being normally distributed, demonstrating that the fit is stable under statistical variations. The yields obtained from the signal extraction fit are shown in Table 2.

The observables, defined in Eqs. 1 and 2 are calculated by the fit, then modified by a set of corrections taken from simulation. The acceptances of $\psi\pi^+$ and ψK^+ events in the detector are computed using PYTHIA [11] to generate the primary

Table 2: Raw fitted yields. The labels ‘D’ and ‘U’ refer to the two polarities of the LHCb dipole.

			B^-	B^+
J/ψ	π	D	528 ± 27	518 ± 27
		U	421 ± 23	428 ± 23
	K	D	$13\,363 \pm 180$	$13\,466 \pm 181$
		U	$10\,666 \pm 148$	$11\,120 \pm 155$
$\psi(2S)$	π	D	94 ± 16	93 ± 16
		U	82 ± 15	70 ± 13
	K	D	$2\,331 \pm 88$	$2\,463 \pm 93$
		U	$2\,026 \pm 78$	$1\,836 \pm 71$

collision and EVTGEN [12] to model the B^+ decay. The efficiency of reconstructing and selecting $\psi\pi^+$ and ψK^+ decays is estimated with a bespoke simulation of LHCb based on GEANT4 [13]. It models the interaction of muons and the two hadron species with the detector material. The total correction $\epsilon^{\psi K}/\epsilon^{\psi\pi}$ is 0.985 ± 0.012 and 1.007 ± 0.021 for $R^{J/\psi}$ and $R^{\psi(2S)}$ respectively.

CP asymmetries are extracted from the observed charge asymmetries (A_{Raw}) by taking account of instrumentation effects. The interaction asymmetry of kaons, A_{Det}^K is expected to be non-zero, especially for low-momentum particles. This asymmetry, measured at LHCb using a sample of $D^{*+} \rightarrow D^0\pi^+$, $D^0 \rightarrow K^+\pi^-$ decays, is -0.010 ± 0.002 if the pion asymmetry is zero [14]. The null-asymmetry assumption for pions has been verified at LHCb to an accuracy of 0.25% [15]. These results are used with enlarged uncertainties (0.004, for both kaons and pions) to account for the different momentum spectra of this sample and those used in the previous analyses.

In summary, the CP asymmetry is defined as

$$A^{\psi h} = A_{\text{Raw}}^{\psi h} - A_{\text{Prod}} - A_{\text{Det}}^h, \quad (4)$$

where the production asymmetry, A_{Prod} , describes the different rates with which B^- and B^+ hadronise out of the pp collisions. The observed, raw charge asymmetry in $B^+ \rightarrow J/\psi K^+$ is -0.012 ± 0.004 . Using Eq. 4 with the established CP asymmetry, $A^{J/\psi K} = 0.001 \pm 0.007$ [3], A_{Prod} is estimated to be -0.003 ± 0.009 . This is applied as a correction to the other modes reported here.

The different contributions to the systematic uncertainties are summarised in Table 3. They are assessed by modifying the final selection,

Table 3: Summary of systematic uncertainties. The statistical fit errors are included for comparison.

	$R^{J/\psi} (\times 10^{-2})$	$A^{J/\psi\pi}$	$R^{\psi(2S)} (\times 10^{-2})$	$A^{\psi(2S)\pi}$	$A^{\psi(2S)K}$
Simulation uncertainty	0.045	-	0.088	-	-
PID efficiencies	0.043	-	0.052	-	-
$A^{J/\psi K}$ (PDG [3])	-	0.0070	-	0.0070	0.0070
$A_{\text{Raw}}^{J/\psi K}$ statistical error	-	0.0046	-	0.0046	0.0046
Detection asymmetries	-	0.0056	-	0.0056	-
Relative trigger efficiency	0.020	0.0031	0.050	0.0036	0.0003
Fixed fit parameters	0.005	0.0006	0.017	0.0013	0.0001
Sum in quadrature (syst.)	0.065	0.0106	0.115	0.0108	0.0084
Fit error (stat.)	0.110	0.0268	0.404	0.0901	0.0136

or altering fixed parameters and rerunning the signal yield fit. The maximum variation of each observable is taken as their systematic uncertainty.

The largest uncertainty is due to the use of simulation to estimate the acceptance and selection efficiencies. It accounts for any bias due to imperfect modelling of the detector and its relative response to pions and kaons. Another important contribution arises from the loose trigger criteria that are employed. This uncertainty is estimated from the shift in the central values after rerunning the fit using only those events where the muons passed the software trigger. The use of the PID calibration to estimate the efficiency for pions to the $DLL_{K\pi} < 6$ selection also contributes a significant systematic uncertainty.

The measurements of $A^{\psi\pi}$ depend on the estimation of A_{Prod} from the $B^+ \rightarrow J/\psi K^+$ channel. The uncertainty on A_{Prod} is determined by the statistical error of $A_{\text{Raw}}^{J/\psi K}$ in the fit, the uncertainty on the world average of $A^{J/\psi K}$ and the estimation of A_{Det}^h . These effects are kept separate in the table where it is seen that the uncertainty on the nominal value of $A^{J/\psi K}$ dominates. Finally, it is noted that the detector asymmetries cancel for $A^{\psi(2S)K}$ and a lower systematic uncertainty can be reported.

The measured ratios of branching fractions are

$$\begin{aligned} R^{J/\psi} &= (3.83 \pm 0.11 \pm 0.07) \times 10^{-2} \\ R^{\psi(2S)} &= (3.95 \pm 0.40 \pm 0.12) \times 10^{-2}, \end{aligned}$$

where the first uncertainty is statistical and the second systematic. $R^{\psi(2S)}$ is compatible with the one existing measurement, $(3.99 \pm 0.36 \pm 0.17) \times 10^{-2}$ [6]. The measurement of $R^{J/\psi}$ is 3.2σ lower than the

current world average, $(5.2 \pm 0.4) \times 10^{-2}$ [3]. Using the established measurements of the Cabibbo-favoured branching fractions [3], we deduce

$$\begin{aligned} \mathcal{B}(B^\pm \rightarrow J/\psi \pi^\pm) &= (3.88 \pm 0.11 \pm 0.15) \times 10^{-5} \\ \mathcal{B}(B^\pm \rightarrow \psi(2S) \pi^\pm) &= (2.52 \pm 0.26 \pm 0.15) \times 10^{-5}, \end{aligned}$$

where the systematic uncertainties are summed in quadrature. The measured CP asymmetries,

$$\begin{aligned} A_{CP}^{J/\psi\pi} &= 0.005 \pm 0.027 \pm 0.011 \\ A_{CP}^{\psi(2S)\pi} &= 0.048 \pm 0.090 \pm 0.011 \\ A_{CP}^{\psi(2S)K} &= 0.024 \pm 0.014 \pm 0.008, \end{aligned}$$

have comparable or better precision than previous results, and no evidence of direct CP violation is seen.

Acknowledgements

We express our gratitude to our colleagues in the CERN accelerator departments for the excellent performance of the LHC. We thank the technical and administrative staff at CERN and at the LHCb institutes, and acknowledge support from the National Agencies: CAPES, CNPq, FAPERJ and FINEP (Brazil); CERN; NSFC (China); CNRS/IN2P3 (France); BMBF, DFG, HGF and MPG (Germany); SFI (Ireland); INFN (Italy); FOM and NWO (The Netherlands); SCSR (Poland); ANCS (Romania); MinES of Russia and Rosatom (Russia); MICINN, XuntaGal and GEN-CAT (Spain); SNSF and SER (Switzerland); NAS Ukraine (Ukraine); STFC (United Kingdom); NSF (USA). We also acknowledge the support received from the ERC under FP7 and the Region Auvergne.

References

- [1] I. Dunietz and J. M. Soares, *Direct CP violation in $b \rightarrow dJ/\psi$ decays*, Phys. Rev. **D49** (1994) 5904, [arXiv:hep-ph/9312233](#).
- [2] J. M. Soares, *More on direct CP violation in $b \rightarrow dJ/\psi$ decays*, Phys. Rev. **D52** (1995) 242, [arXiv:hep-ph/9404336](#).
- [3] Particle Data Group, K. Nakamura *et al.*, *Review of particle physics*, J. Phys. **G37** (2010) 075021.
- [4] BaBar collaboration, B. Aubert *et al.*, *Study of $B^\pm \rightarrow J/\psi\pi^\pm$ and $B^\pm \rightarrow J/\psi K^\pm$ decays: Measurement of the ratio of branching fractions and search for direct CP violation*, Phys. Rev. Lett. **92** (2004) 241802, [arXiv:hep-ex/0401035](#).
- [5] D0 collaboration, V. Abazov *et al.*, *Study of direct CP violation in $B^\pm \rightarrow J/\psi K^\pm(\pi^\pm)$ decays*, Phys. Rev. Lett. **100** (2008) 211802, [arXiv:0802.3299](#).
- [6] Belle collaboration, V. Bhardwaj *et al.*, *Observation of $B^\pm \rightarrow \psi(2S)\pi^\pm$ and search for direct CP-violation*, Phys. Rev. **D78** (2008) 051104, [arXiv:0807.2170](#).
- [7] LHCb collaboration, A. A. Alves Jr *et al.*, *The LHCb detector at the LHC*, JINST **3** (2008) S08005.
- [8] W. D. Hulsbergen, *Decay chain fitting with a Kalman filter*, Nucl. Instrum. Meth. **A552** (2005) 566, [arXiv:physics/0503191](#).
- [9] W. Verkerke and D. Kirkby, *The RooFit toolkit for data modeling*, [arXiv:physics/0306116](#).
- [10] T. Skwarnicki, *A study of the radiative cascade transitions between the Upsilon-prime and Upsilon resonances*. PhD thesis, Institute of Nuclear Physics, Krakow, 1986, DESY-F31-86-02.
- [11] T. Sjöstrand, S. Mrenna, and P. Skands, *PYTHIA 6.4 physics and manual*, JHEP **05** (2006) 026, [arXiv:hep-ph/0603175](#).
- [12] D. J. Lange, *The EvtGen particle decay simulation package*, Nucl. Instrum. Meth. **A462** (2001) 152.
- [13] GEANT4 collaboration, S. Agostinelli *et al.*, *GEANT4: A simulation toolkit*, Nucl. Instrum. Meth. **A506** (2003) 250.
- [14] LHCb collaboration, R. Aaij *et al.*, *First evidence of direct CP violation in charmless two-body decays of B_s^0 mesons*, [arXiv:1202.6251](#), submitted to Phys. Rev. Lett.
- [15] LHCb collaboration, R. Aaij *et al.*, *Measurement of the $D_s^+ - D_s^-$ production asymmetry*, LHCb-PAPER-2012-009.